

Nuclear longitudinal structure function in eA processes at the LHeC

G.R.Boroun,^{*} B.Rezaei,[†] and S.Heidari

Physics Department, Razi University, Kermanshah 67149, Iran

(Dated: April 18, 2018)

The nucleon and nuclear longitudinal structure functions are determined by the Kharzeev-Levin-Nardin (KLN) model of the low x gluon distribution. The behavior of the gluon distribution ratio $R_g = \frac{G^A}{AG^p}$ and the ratio $R_L^{total} = \frac{F_L^{A-total}}{AF_L^{p-total}}$ in this processes are found. The heavy longitudinal structure function ratios $R_L^H = \frac{F_L^{H(A)}}{AF_L^H(p)}$ in eA processes at the LHeC region are discussed. Heavy contributions to the total longitudinal structure function ratio R_L^H are considerable and should not be neglected especially at smaller x of the LHeC project. In the KLN model the new geometrical scaling for transition from the linear to nonlinear regions in accordance with the LHeC processes is used, whose results intensively depended on the heavy quarks mass effect.

I. Introduction

Our knowledge of the gluon distribution function of free nucleons comes from the deep inelastic scattering (DIS) measurements in lepton-nucleon collisions, as at low- x the gluon distributions are predominant at all values of Q^2 . There is a transition from the linear to the nonlinear regions as it can be tamed by screening effects. These nonlinear terms reduce the growth of the gluon distribution at low x values. Therefore DIS processes in LHeC provides very important tools for probing the gluon distribution in the nucleons and in the nuclei. The nuclear gluon distribution $xg^A(x, Q^2)$ can be determined from the gluon distribution of nucleons bound in a nucleus. In addition, the nuclear distribution functions can be extracted from the measurements of deeply inelastic lepton-nucleus scattering (eA processes). In the electron-proton/ion collider LHeC, we intend to demonstrate how the low x data are possible for nuclear targets and could constrain the nuclear gluon distribution function.

The LHeC shows an increase in the kinematic range of the deep inelastic scattering (DIS) as the DIS kinematics are $2 < Q^2 < 100,000 \text{ GeV}^2$ and $0.000002 < x < 0.8$ with a center-of-mass energy of about $\sqrt{s_{ep}} > 1 \text{ TeV}$. Clearly this increase in the precision of parton distribution functions (PDF's) at low- x kinematic region is expected to appear due to the non-linear effects in the so-called saturation region [1-4].

The nuclear parton distribution functions (nPDF's) on the scales Q^2 can be determined based on the DGLAP [5-6] evolution, analogously to the parton distributions of the free proton. At low x , the data show a reduction of the nuclear distribution functions

with respect to the free distribution functions. This phenomenon is caused by the nuclear shadowing effects as $xg^A(x, Q^2) < Axg^N(x, Q^2)$. These shadowing corrections give rise to the nonlinear terms in the evolution equation for the gluon distribution function. Indeed, these behaviors are tamed due to the saturation effects. In the gluon saturation approach, an important point is the x -dependence saturation scale $Q_s^2(x)$ where it is the critical line between the linear and nonlinear regions. For $Q^2 > Q_s^2(x)$, it is expected that the nonlinear effects should be weak and for $Q^2 < Q_s^2(x)$ the nonlinear effects should be strong which generate geometrical scaling in this region. This scaling argument leads to that σ_{γ^*A} dependence on one dimensionless variable τ_0 as $\sigma_{\gamma^*A}(\tau_0)$ and $\tau_0 = \frac{Q^2}{Q_s^2(x)}$ where the saturation scale is given by $Q_s^2(x) = Q_0^2(\frac{x}{x_0})^{-\lambda}$ [7-9]. Here $Q_0^2 = 0.34 \text{ GeV}^2$ and $x_0 = 3.0 \times 10^{-3}$ and exponent λ is a dynamical quantity of the order $\lambda \simeq 0.25$.

The paper is organized as follows: Section II deals with KLN model in transition from traditional geometrical scaling to new geometrical scaling with respect to the heavy quarks mass. Section III introduces the nuclear longitudinal structure function with considering the heavy quarks portion. In section IV we finalized the total longitudinal structure function calculation for light and heavy nuclei. Finally, in Sec.V we summarized the results.

II. KLN model and saturation scale

We focus on the nuclear longitudinal structure function based on the geometrical scaling at low x . The main purpose of this study is to analyze possible compatibility of the new geometrical scaling with the KLN model for transition from the nuclear linear to nonlinear behaviors. In heavy production, geometrical scaling is expected to

^{*}Electronic address: grboroun@gmail.com; boroun@razi.ac.ir

[†]brezaei@razi.ac.ir

be violated due to large heavy quarks mass, as the traditional geometrical scaling (τ_0) one can modify to take account the heavy quark mass [9]:

$$\tau_H = (1 + \frac{4m_H^2}{Q^2})^{1+\lambda} \frac{Q^2}{Q_0^2} (\frac{x}{x_0})^\lambda. \quad (1)$$

In the KLN model [10], a simple relation for the unintegrated gluon distribution was observed as it is related to the gluon distribution by the following form

$$G(x, Q^2) = \int^{Q^2} dk_t^2 \varphi(x, k_t^2), \quad (2)$$

where φ is the unintegrated gluon distribution of a nucleon or nucleus. Authors in Ref.[10] used a simplified assumption about the form of $G(x, Q^2)$ by two regions of integration over Q^2 defined along the critical line Q_s^2 . For a nucleon we shall use the KLN Ansatz as

$$G(x, Q^2) = \begin{cases} \frac{K_0 S}{\alpha_s(Q_s^2)} Q^2 (1-x)^4, & Q^2 < Q_s^2 (\tau_0 < 1) \\ \frac{K_0 S}{\alpha_s(Q_s^2)} Q_s^2 (1-x)^4, & Q^2 > Q_s^2 (\tau_0 > 1), \end{cases} \quad (3)$$

where the numerical coefficient K_0 can be determined from gluon density, which is usually taken from the parameterization groups and S is the area corresponding to target. Here the factor $(1-x)^4$ is to describe the fact that the gluon density is small at high x values.

For a nucleus with the mass number A , the gluon distribution function $G(x, Q^2)$ changed to $G^A(x, Q^2)$ with replacements $S \rightarrow S^A = A^{\frac{2}{3}} S$ and $Q_s^2 \rightarrow Q_s^{2A} = A^{\frac{1}{3}} Q_s^2$ [11]. The gluon distribution for a nucleus with respect to Eq.3 can be written as

$$G^A(x, Q^2) = \begin{cases} \frac{K_0 S^A}{\alpha_s(Q_s^{2A})} Q^2 (1-x)^4, & Q^2 < Q_s^{2A} (\tau_0^A < 1) \\ \frac{K_0 S^A}{\alpha_s(Q_s^{2A})} Q_s^{2A} (1-x)^4, & Q^2 > Q_s^{2A} (\tau_0^A > 1). \end{cases} \quad (4)$$

The transition point between the linear and nonlinear regions along the critical line for the proton ($A = 1$) and a nucleus (A) is

$$x_c = x_0 (\frac{Q_0^2 A^{1/3}}{Q^2})^{1/\lambda}. \quad (5)$$

Table.1 shows that the critical point is dependent on the mass number A and the values of Q^2 . At low x values, the transition point between the linear and nonlinear behavior is observable for light nuclei at low Q^2 and for heavy nuclei at low and moderate Q^2 values in eA processes. These critical points refer to zero quark mass such as the geometrical scaling defined by $\tau_0^A (= \frac{Q^2}{Q_s^{2A}(x)})$. Since masses of heavy quarks in the LHeC region are not negligible, therefore the geometrical scaling is expected to be violated than dimensionless quantity τ_0 . With respect to this new geometrical scaling $\tau_H^A (= (1 + \frac{4m_H^2}{Q^2})^{1+\lambda} \frac{Q^2}{Q_s^{2A}})$ in Eqs.3 and 4, the transition points shift to low x values

as transition between the linear and nonlinear behaviors tamed at low x values. These critical points introduced by the following form

$$x_c = x_0 (\frac{Q_0^2 A^{1/3}}{Q^2 (1 + \frac{4m_H^2}{Q^2})})^{1/\lambda}, \quad (6)$$

and observed in Table 2-4 to take into account m_H . Indeed, the difference between the (traditional) geometrical scaling variable (τ_0) and the "new" geometrical scaling variable (τ_H), particularly for eA (who is τ_0^A and τ_H^A) strongly dependence to the heavy quark mass as $\frac{\Delta\tau}{\tau_0}$ or $\frac{\Delta\tau^A}{\tau_0^A} = (1 + \frac{4m_H^2}{Q^2})^{1+\lambda} - 1$.

Fig.1 shows the behavior of the ratio $R_g = \frac{G^A(x, Q^2)}{AG^p(x, Q^2)}$ for light and heavy nuclei $A = 12$ and $A = 208$ respectively at Q^2 values of 2, 10 and 100 GeV^2 in order to determine the gluon densities in nuclei. The magnitude of shadowing effects are considered by the geometrical scaling behavior at low x values. By the traditional scaling we observe the saturation effects for the ratio R_g at $x < 10^{-2}$ and for small values of Q^2 at light and high nuclei. As expected, with new geometrical scaling this critical point is noticeable at $x < 10^{-5}$ until $x < 10^{-15}$ in accordance with heavy quarks mass respectively (see Figs.2-3). These observations are essential in the ratios when we take into account heavy quarks mass.

III. Nuclear longitudinal structure function

Now, we consider the nuclear longitudinal structure function at eA processes with respect to the nuclear gluon density behavior. The nuclear longitudinal structure function is interest since it is directly sensitive to the nuclear gluon density through the transition $g^A \rightarrow q^A \bar{q}^A$ in eA -DIS. Indeed a measurement of $F_L^A(x, Q^2)$ can be used to extract the nuclear gluon structure function and therefore the measurement of F_L^A provides a sensitive test of perturbative QCD (pQCD). Since the longitudinal structure function F_L contains rather large heavy flavor contributions in the small- x region, therefore the measurements of these observables in the eA processes have told us about the portion of the heavy quarks contribution to the nuclear longitudinal structure function and also the dependence of nuclear parton distribution functions (nPDFs) on heavy quarks masses. In perturbative QCD, the nuclear longitudinal structure function can be written as

$$x^{-1} F_L^A = C_{L,ns} \otimes q_{ns}^A + e^2 > (C_{L,q} \otimes q_s^A + C_{L,g} \otimes g^A) + x^{-1} F_L^{Heavy-A}. \quad (7)$$

The symbol \otimes represents the common convolution as its given by, $A(x) \otimes B(x) = \int_x^1 \frac{dy}{y} A(y) B(\frac{x}{y})$, and q_{ns}^A, q_i^A and

g^A represent the number distributions of quarks and gluons in nuclei, respectively. $\langle e^2 \rangle$ is the average squared charge ($= \frac{2}{9}$ for light quarks) and $C_{L,a}$ is the perturbative expansion of the coefficient functions as it can be written

$$C_{L,a}(\alpha_s, x) = \sum_{n=1} \left(\frac{\alpha_s}{4\pi}\right)^n c_{L,a}^{(n)}(x). \quad (8)$$

At low x , the gluon contribution to the total nuclear longitudinal structure function dominates over the singlet and nonsinglet contribution as

$$F_L^A|_{x \rightarrow 0} \simeq F_L^{g-A} + F_L^{Heavy-A}. \quad (9)$$

The gluonic nuclear longitudinal structure function is given by

$$F_L^{g-A}(x, Q^2) = \sum_{n=1} \left(\frac{\alpha_s}{4\pi}\right)^n \langle e^2 \rangle c_{L,g}^{(n)}(x) \otimes G^A(x, Q^2), \quad (10)$$

and $F_L^{Heavy-A}$ at low x is depended on nuclear gluon distribution when neglecting the contributions due to incoming light quarks and anti-quarks in boson gluon fusion. Therefore

$$\begin{aligned} F_L^{Heavy-A}(x, Q^2) &= C_{L,g}^{Heavy}(x, Q^2) \otimes G^A(x, Q^2) \\ &\equiv \sum_{n=1} F_L^{(n), Heavy-A}(x, Q^2), \end{aligned} \quad (11)$$

where n is the order of α_s . At low x , Eqs.10 and 11 explicitly are dependent to the strong coupling constant and nuclear gluon density.

Similarly, in the electron-proton collision, the gluonic longitudinal structure function is directly dependence to the gluon distribution function as some analytical solutions of the Altarelli- Martinelli equation [13] using the expanding method and hard pomeron behavior initialized

by Cooper-Sarkar *et al.*, have been reported in last years [14-15] with considerable phenomenological success. At leading order analysis (LO), the gluonic nuclear longitudinal structure function is given by

$$\begin{aligned} F_L^{g-A}(x, Q^2) &= \frac{\alpha_s}{4\pi} \left[\sum_{i=1}^{N_f} e_i^2 \right] \int_x^1 \frac{dy}{y} [8(x/y)^2(1-x/y)] \\ &\quad \times G^A(y, Q^2), \end{aligned} \quad (12)$$

and

$$\begin{aligned} F_L^{Heavy-A}(x, Q^2) &= F_L^{c-A}(x, Q^2) + F_L^{b-A}(x, Q^2) \\ &\quad + F_L^{t-A}(x, Q^2), \end{aligned} \quad (13)$$

where

$$\begin{aligned} F_L^{Heavy-A}(x, Q^2, m_H^2) &= 2e_H^2 \frac{\alpha_s(\mu_H^2)}{2\pi} \int_{x a_H}^1 \frac{xdy}{y^2} \\ &\quad \times C_{L,g}^H\left(\frac{x}{y}, \frac{m_H^2}{Q^2}\right) G^A(y, \mu_H^2). \end{aligned} \quad (14)$$

Here $a_H = 1 + 4\frac{m_H^2}{Q^2}$, $C_{L,g}^H$ is the heavy coefficient function related to the heavy quarks masses and the scale $\mu_H (= \sqrt{\frac{Q^2}{2} + 4m_H^2})$ is the mass factorization and the renormalization scale. $\alpha_s(\mu_H^2)$ is the running coupling constant and the heavy longitudinal coefficient function can be expressed as

$$C_{L,g}^H(z, \zeta) = -4z^2 \zeta_H \ln \frac{1+\beta_H}{1-\beta_H} + 2\beta_H z(1-z), \quad (15)$$

where $\beta_H^2 = 1 - \frac{4z\zeta_H}{1-z} (\zeta_H \equiv \frac{m_H^2}{Q^2})$.

Exploiting the low- x behavior of the nuclear gluon distribution function according to the KLN model, therefore the behavior of the $F_L^{A-total}$ denoted by

$$\begin{aligned} F_L^{A-total} &= \frac{\alpha_s}{4\pi} \left[\sum_{i=1}^{N_f} e_i^2 \right] \int_x^1 \frac{dy}{y} [8(x/y)^2(1-x/y)] G^A(y, Q^2) + 2e_c^2 \frac{\alpha_s(\mu_c^2)}{2\pi} \int_{a_{cx}}^1 \frac{xdy}{y^2} C_{L,g}^c\left(\frac{x}{y}, \zeta_c\right) G^A(y, \mu_c^2) \\ &\quad + 2e_b^2 \frac{\alpha_s(\mu_b^2)}{2\pi} \int_{a_{bx}}^1 \frac{xdy}{y^2} C_{L,g}^b\left(\frac{x}{y}, \zeta_b\right) G^A(y, \mu_b^2) \\ &\quad + 2e_t^2 \frac{\alpha_s(\mu_t^2)}{2\pi} \int_{a_{tx}}^1 \frac{xdy}{y^2} C_{L,g}^t\left(\frac{x}{y}, \zeta_t\right) G^A(y, \mu_t^2). \end{aligned} \quad (16)$$

As shown in Fig.1, the behavior of the ratio $R_L = \frac{F_L^{g-A}}{AF_L^{g-p}}$ as a function of x for $Q^2 = 2, 10$ and 100 GeV^2 and nuclei $A = 12$ and $A = 208$ is presented. The transition point between the linear and nonlinear regions are

shown at low Q^2 values in this figure. These results are comparable with EKS [16] and EPS [17] analysis in comparison with DS [18] and HKN [19] parameterizations at low x and also with nuclear PDFs from the LHeC perspective [20]. The magnitude of the shadowing

effect is dependence to the Q^2 values and A . In fact, this model predict a large value of shadowing at low and high Q^2 values. The shadowing effects for heavy nuclei are larger than light nuclei at a wide range of x and Q^2 . Figures 2-3 show the transition point between linear and nonlinear regions with respect to the new geometrical scaling shifted towards very low x values, and this is related to the nuclear mass in eA processes.

In Figs.4-5, we present the small- x behavior of the ratio R_L^H according to the traditional transition point (Eq.5) as a function of x for $Q^2 = 2, 10$ and 100 GeV^2 and nuclei $A = 12$ and $A = 208$. In these figures we observed antishadowing and shadowing behaviors at low x and low Q^2 values in accordance with the traditional geometrical scaling (Eq.5). In all the cases, the depletion and enhancement in these ratios reflecting the linear(at $x > x_c$)/linear(at $x > x_c$), nonlinear(at $x < x_c$)/linear(at $x > x_c$) and nonlinear(at $x < x_c$)/nonlinear(at $x < x_c$) behavior for nuclei/nucleon related to Eq.5. The enhancement in the ratio nuclei/nucleon, as it is called antishadowing, is related to the nonlinear behavior for nuclei. Because nuclei transition from linear to nonlinear regions is quickly than nucleon (i.e., nuclei(nonlinear at $x < x_c$)/nucleon (linear at $x > x_c$)).

Now, the new transition points for these ratios are shown in figures 6-7 in accordance with Eq.6 for charm, bottom and top quarks. Indeed the nonlinear effects are predominant for light and heavy nuclei at low- Q^2 values. In fact the shadowing effects for $A = 12$ are observable at $Q^2 = 2 \text{ GeV}^2$ and $x < 10^{-6}$ and for $A = 208$ are observable at $Q^2 = 2$ and 10 GeV^2 at $x < 10^{-5}$ by the charm content of the nuclei and nucleon. For bottom and top contribution to the longitudinal structure functions the shadowing effects will be noticeable at $x < 10^{-7}$ and low Q^2 values, which may be expected to be predicted at LHeC energies.

A comparison between R_L (Fig.1) and R_L^H (Figs.6-7) shows that transition point for going to the shadowing region is at larger values of x . This is consistent with light and heavy quarks mass.

IV. Total longitudinal structure function

Let us now discuss the ratio of the total longitudinal structure functions. It is well known that the inclusive observable F_L^{total} is strongly dependent on the gluon distribution for gluonic and heavy contributions to the structure function. Fig.8 shows the results for the total longitudinal structure function ratio at $A = 12$ and $A = 208$ and at Q^2 value of 2 GeV^2 where saturation effect is observable than other Q^2 values. In this value of Q^2 , the significant nonlinear effects is observable as this effect start to appear at $x \leq 10^{-3}$ for heavy nuclei and decrease to lower x values for light nuclei. For light and

heavy nuclei, the shadowing effect is observable at low x values. An enhancement at the behavior of the ratio for light nuclei (in Fig.8 on the left panel) is due to the KLN gluon model and may be due to the anti-shadowing effects. The ratio of the total longitudinal structure function decreases as A increases.

V. Summary

In conclusion, we have observed that the KLN model for the total longitudinal structure function ratio R_L^{total} gives the saturation effect of the heavy quarks effects to the light flavors at small x . This ratio shows shadowing for heavy nuclei at low x and also for light nuclei where shows an enhancement in addition to a depletion at this region. The results are close to EPS nuclear distribution. Lastly, one important conclusion is that heavy contribution to total longitudinal structure function ratio $R_L^{total} = \frac{F_L^{A-total}}{AF_L^{p-total}}$ is considerable one and cannot be neglected especially at smaller x of the LHeC project.

Acknowledgments

We thank F.O.Durães for useful discussions, comments and reading the manuscript.

REFERENCES

1. LHeC workshops 2015 (<http://cern.ch/lhec>).
2. G.R.Boroun, Phys.Lett.B**744** (2015)142; Phys.Lett.B**741** (2015)197.
3. J.L.Abelleira Fernandez, et.al., [LHeC Collab.], J.Phys.G**39** (2012)075001.
4. M.Klein, Ann.Phys. **528**,No.1-2(2016)138-144.
5. V.N. Gribov and L.N. Lipatov, Sov. J. Nucl. Phys.**18** (1972) 438.
6. L.N. Lipatov, Sov. J. Nucl. Phys.**20** (1975) 93; G. Altarelli and G. Parisi, Nucl. Phys. B**126** (1977) 298; Yu.L. Dokshitzer, Sov. Phys. JETP **46** (1977) 641.
7. M.Praszalowicz and T.Stebel, JHEP 04 (2013) 169.
8. G.Beuf and D.Royon, arXiv:hep-ph/0810.5082(2008).
9. T.Stebel, Phys. Rev. D **88** (2013), 014026.
10. D.Kharzeev, E.Levin and M.Nardi, Nucl.Phys.A**730** (2004)448;Nucl.Phys.A**747** (2005)609.
11. F.Carvalho, F.O.Durães, F.S.Navarra and S.Szpigel, Phys.Rev.C**79** (2009)035211.
12. E.R.Cazaroto, F.Carvalho. V.P.Goncalves and F.S.Navarra, Phys.Lett.B**669** (2008)331.
13. G.Altarelli and G.Martinelli, Phys.Lett.B**76**

TABLE I: Critical point x_c along the critical line $Q_s^2 = Q^2$.

$Q^2(GeV^2)$	$x_c^{A=1}$	$x_c^{A=12}$	$x_c^{A=208}$
2	0.25E-5	0.70E-4	0.31E-2
10	0.40E-8	0.11E-6	0.50E-5
100	0.40E-12	0.11E-10	0.50E-9

TABLE II: Critical point x_c with new geometrical scaling to take into account m_c .

$Q^2(GeV^2)$	$x_c^{A=1}$	$x_c^{A=12}$	$x_c^{A=208}$
2	0.41E-8	0.12E-6	0.51E-5
10	0.50E-9	0.14E-7	0.61E-6
100	0.31E-12	0.85E-11	0.39E-9

(1978)89.

14. A.M.Cooper-Sarkar et al., Z.Phys.C**39** (1998)281.15. G.R.Boroun and B.Rezaei, Eur. Phys. J. C**72** (2012)2221.16. K.J.Eskola, V.J.Kolhinen and C.A.Salgado, Eur.Phys.J.C**9** (1999)61.17. K.J.Eskola, H.Paukkunen and C.A.Salgado, JHEP**0807** (2008)102.18. D.de Florian and R.Sassto, Phys.Rev.D**69** (2004)074028.19. M.Hirai, S.Kumano and T.H.Nagai, Phys.Rev.C**76** (2007) 065207.

20. H.Paukkunen, K.J.Eskola and N.Armesto, arXiv:hep-ph/1306.2486(2013).

21.E.R.Cazaroto, F.Carvalho. V.P.Goncalves and F.S.Navarra, Phys.Lett.B**671** (2009)233.TABLE IV: The same Table 2 with m_t .

$Q^2(GeV^2)$	$x_c^{A=1}$	$x_c^{A=12}$	$x_c^{A=208}$
2	0.81E-18	0.22E-16	0.99E-15
10	0.38E-17	0.10E-15	0.47E-14
100	0.20E-16	0.54E-15	0.24E-13

Figure Captions

Fig.1. R_g and R_L evaluated as a function of x for $Q^2 = 2, 10$ and $100 GeV^2$ at nuclei $A = 12$ and $A = 208$ with the KLN model.

Fig.2. R_g and R_L evaluated as a function of the geometrical scalings at $Q^2 = 2 GeV^2$ for the nuclear $A = 12$.

Fig.3. The same Fig.2 for $A = 208$.

Fig.4. The ratio $R_L^H = \frac{F_L^{H(A)}}{AF_L^{H(p)}}$ for $A = 12$ at $Q^2 = 2, 10$ and $100 GeV^2$.

Fig.5. The same Fig.4 for $A = 208$.

Fig.6. The nonlinear and shadowing behavior of the R_L^H for $A = 12$ in accordance with new geometrical transition point.

Fig.7. The same Fig.6 for $A = 208$.

Fig.8. R_L^{total} for $A = 12$ and $A = 208$ at $Q^2 = 2 GeV^2$.

TABLE III: The same Table 2 with m_b .

$Q^2(GeV^2)$	$x_c^{A=1}$	$x_c^{A=12}$	$x_c^{A=208}$
2	0.23E-10	0.64E-9	0.29E-7
10	0.22E-10	0.61E-9	0.27E-7
100	0.17E-12	0.48E-11	0.21E-9

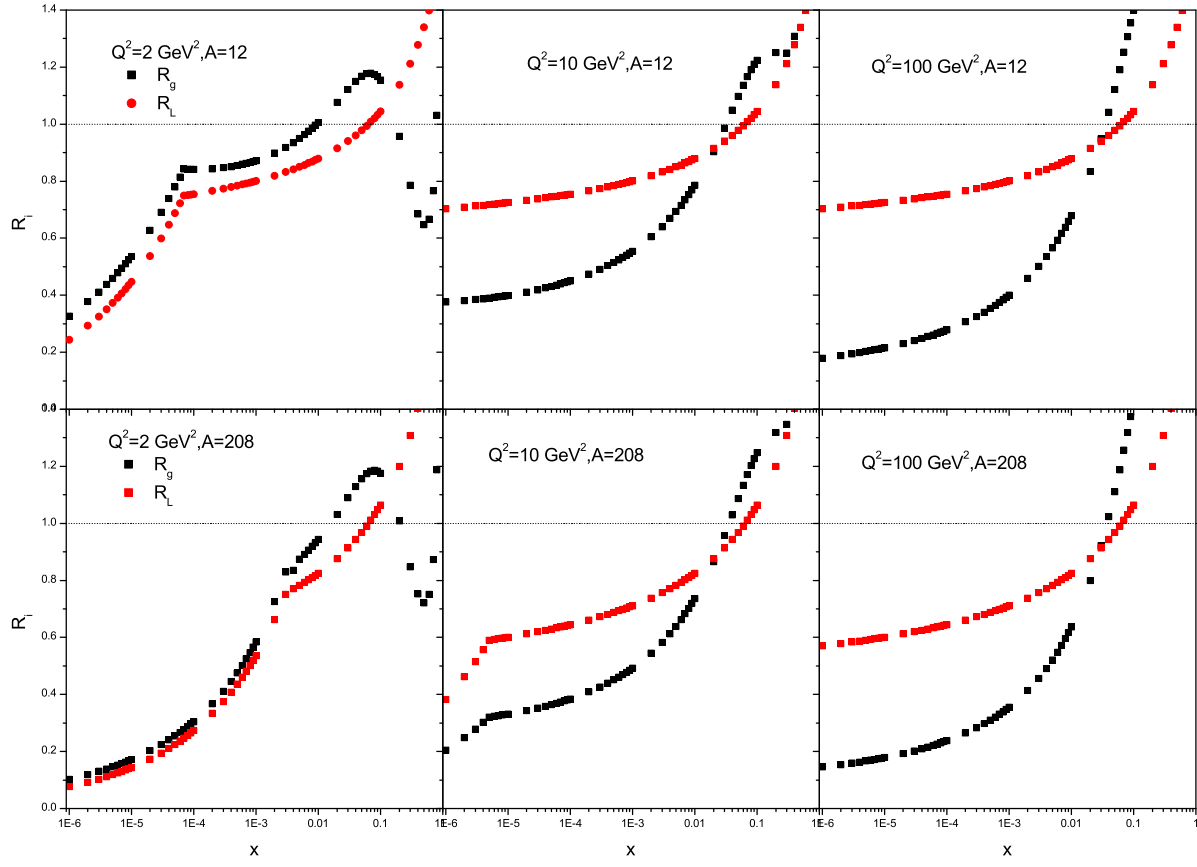


Fig.1

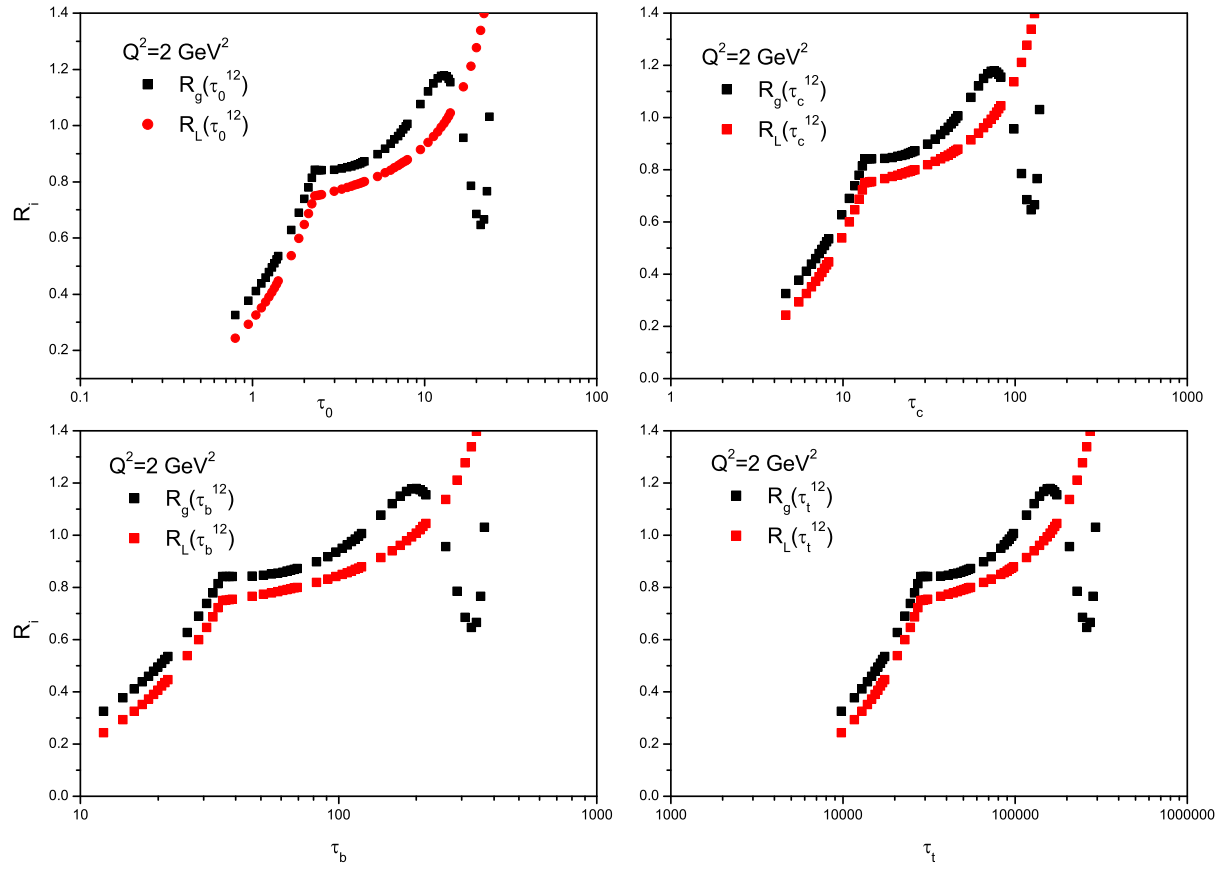


Fig.2

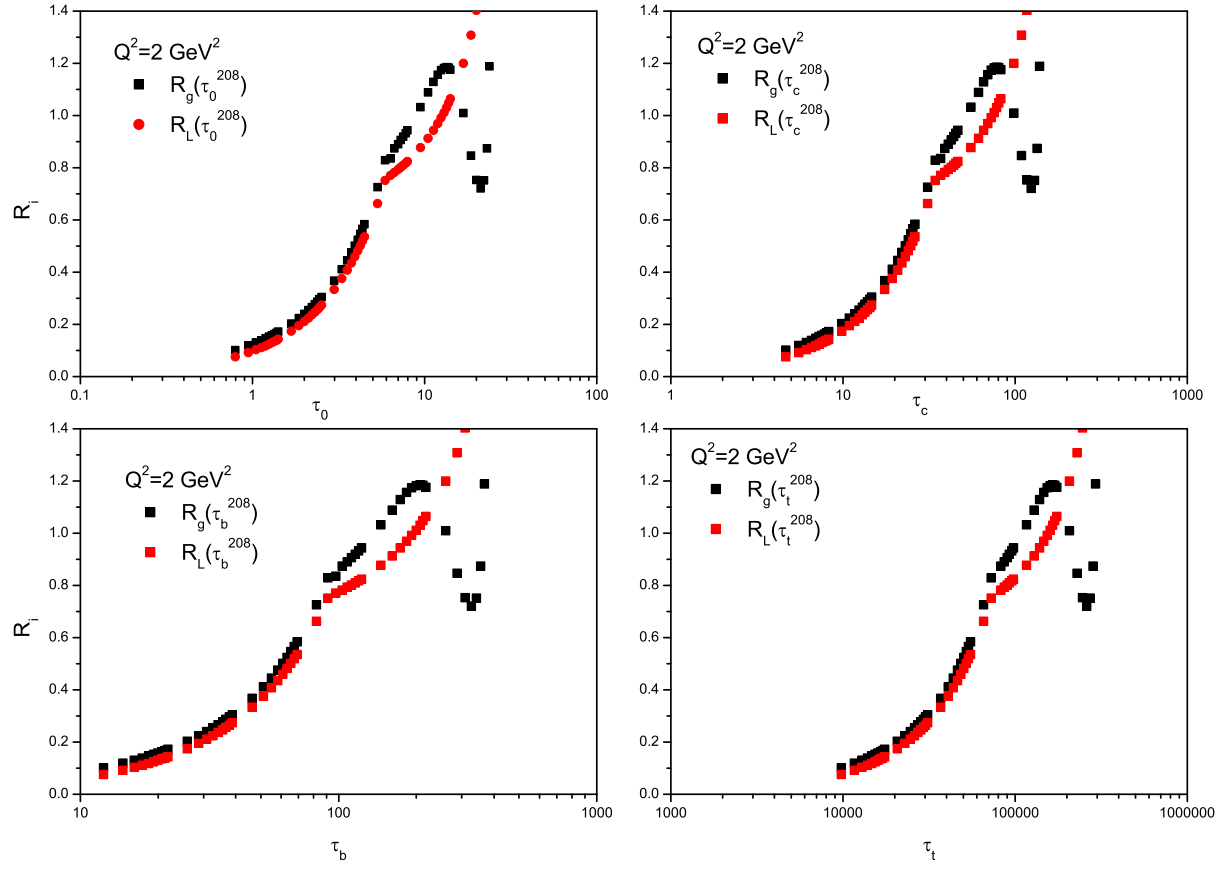


Fig.3

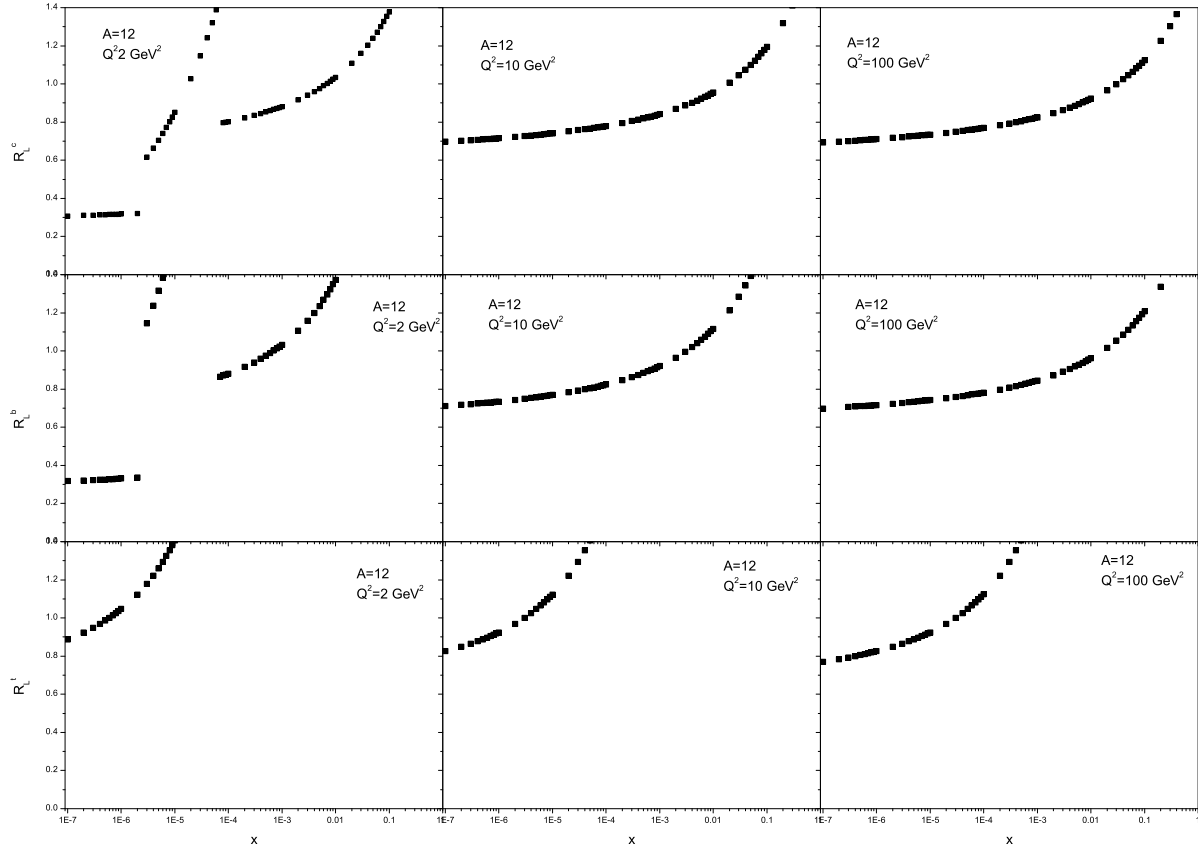


Fig.4

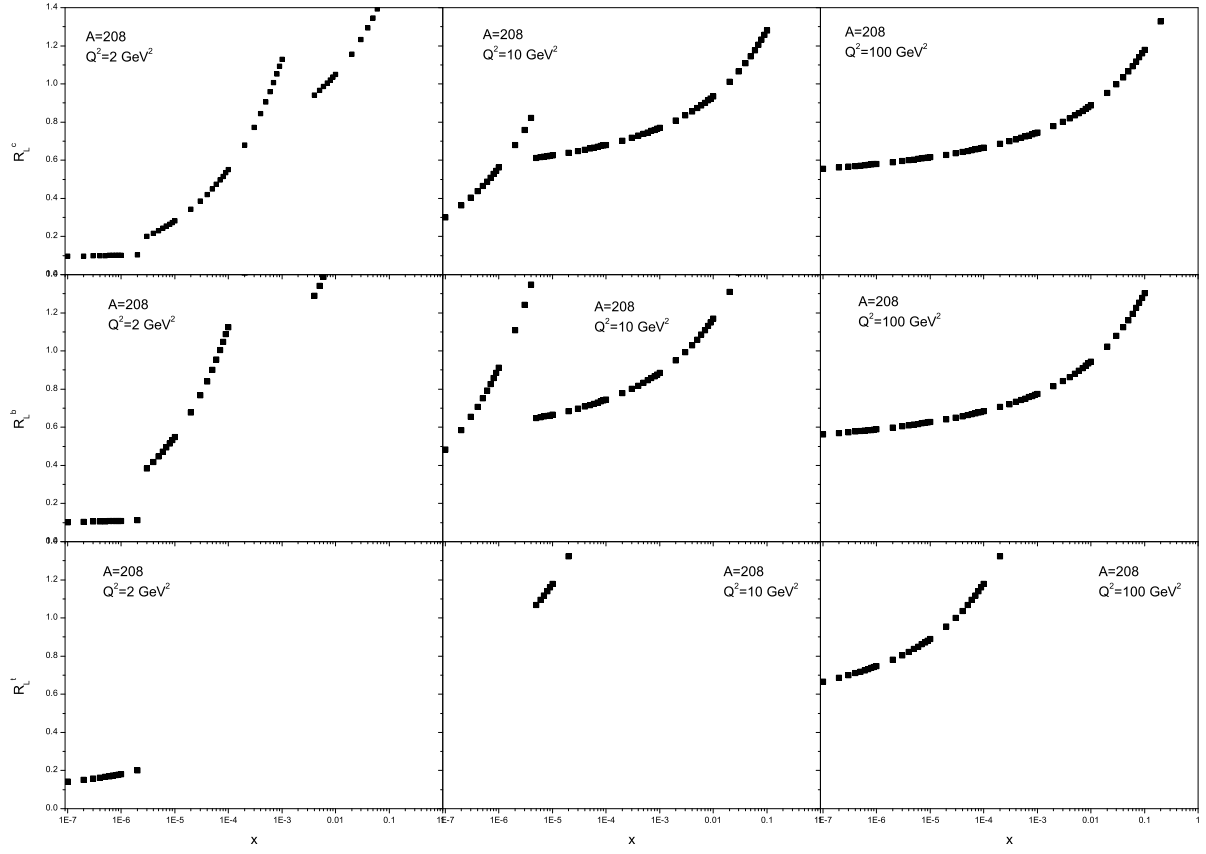


Fig.5

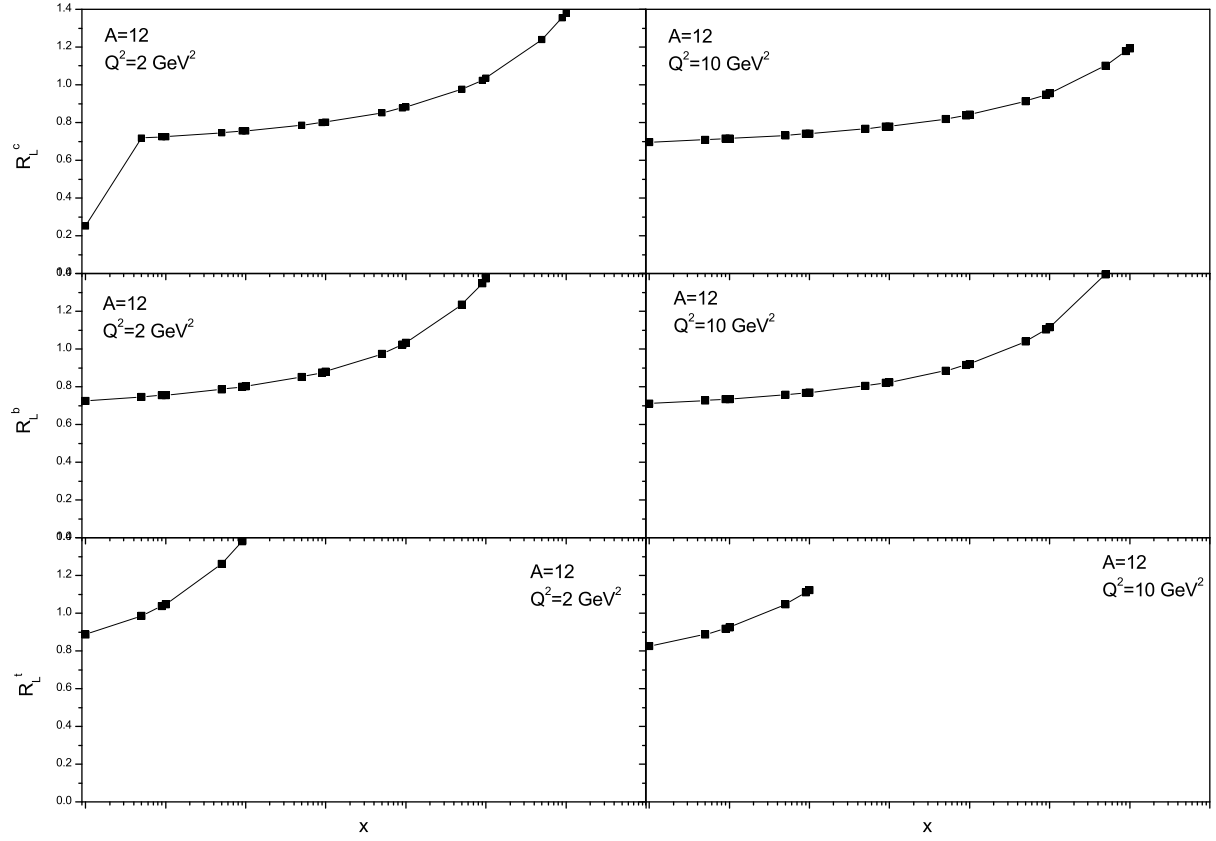


Fig.6

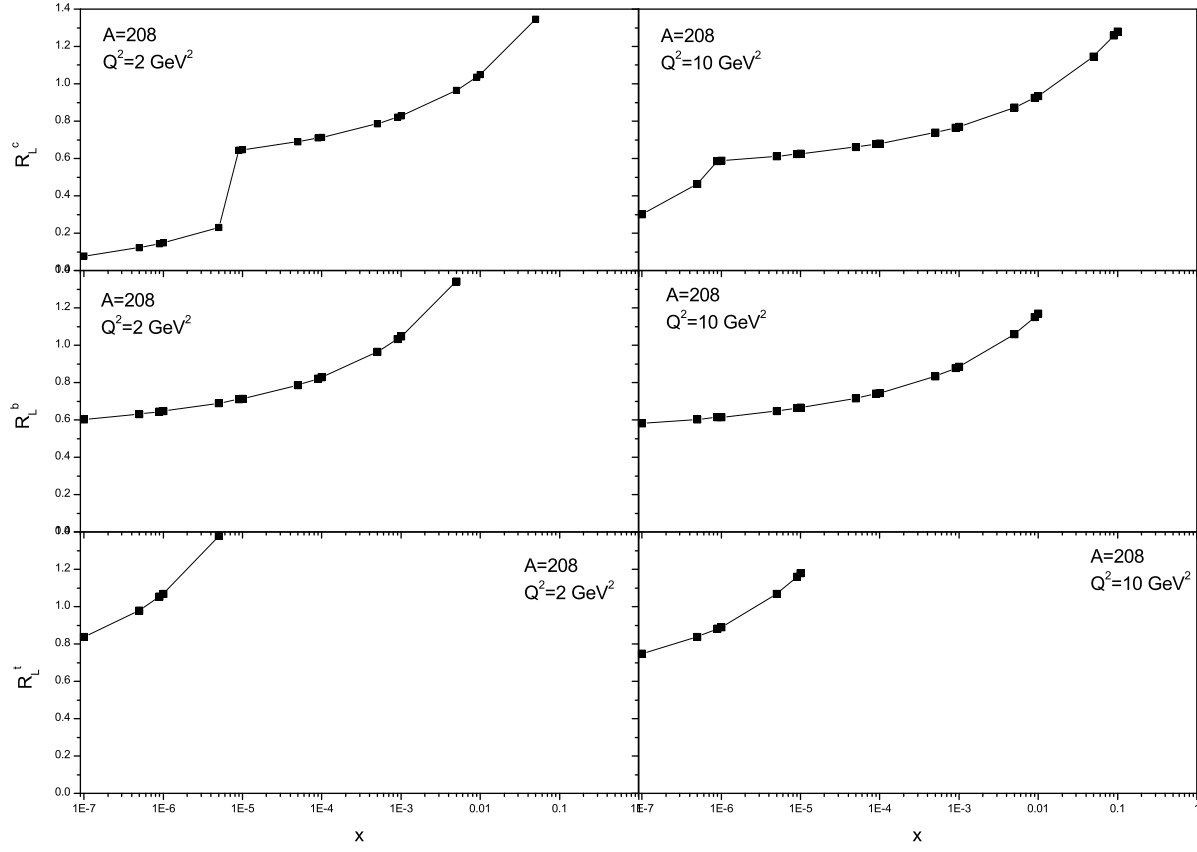


Fig.7

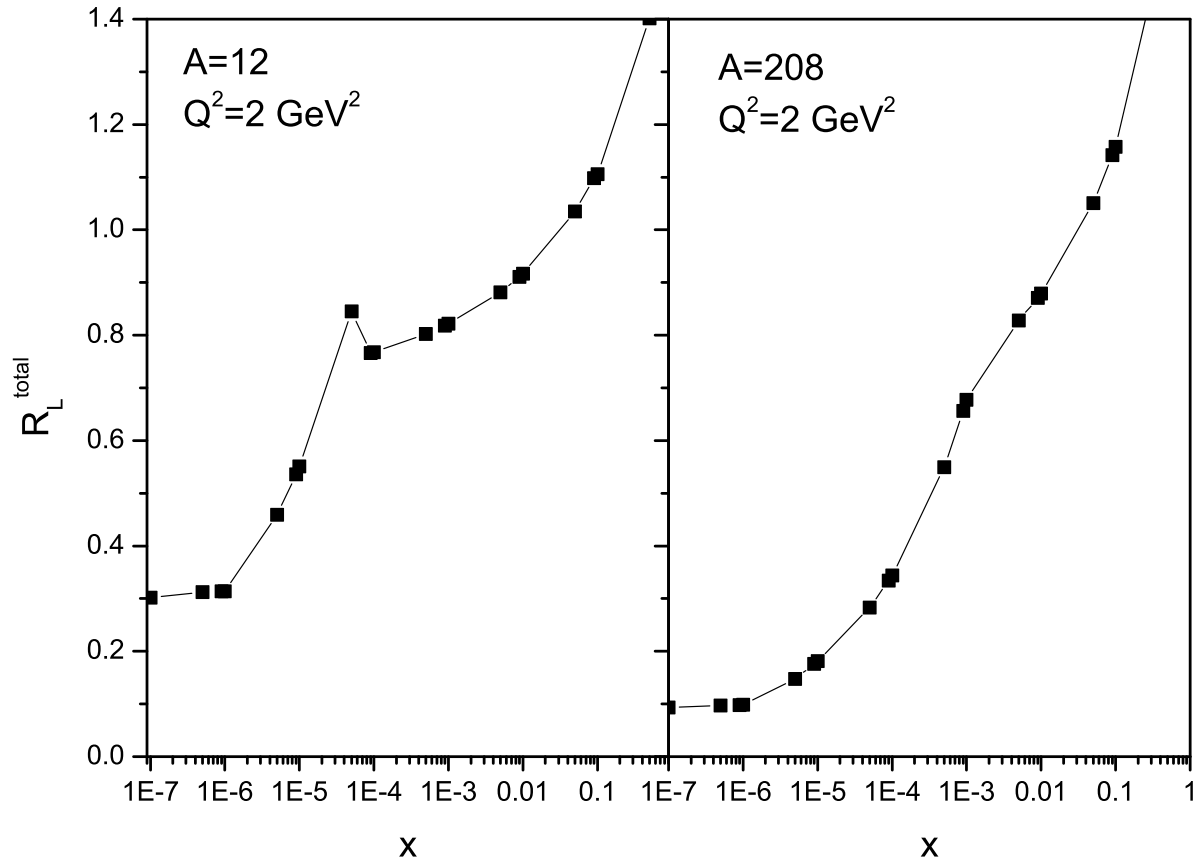


Fig.8